CrossMark
click for updates

View Article Online
View Journal

# Organic & Biomolecular Chemistry

## Accepted Manuscript

This article can be cited before page numbers have been issued, to do this please use: S. K. Albert, M. Golla, H. V. P. Thelu, N. Krishnan, P. Deepak and R. Varghese, *Org. Biomol. Chem.*, 2016, DOI: 10.1039/C6OB00681G.

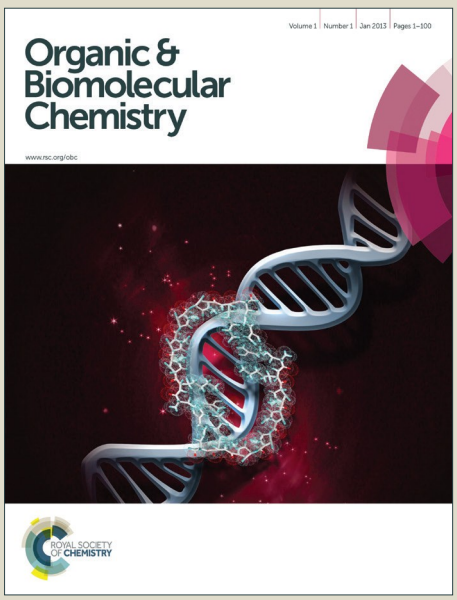


This is an *Accepted Manuscript*, which has been through the Royal Society of Chemistry peer review process and has been accepted for publication.

*Accepted Manuscripts* are published online shortly after acceptance, before technical editing, formatting and proof reading. Using this free service, authors can make their results available to the community, in citable form, before we publish the edited article. We will replace this *Accepted Manuscript* with the edited and formatted *Advance Article* as soon as it is available.

You can find more information about *Accepted Manuscripts* in the Information for Authors.

Please note that technical editing may introduce minor changes to the text and/or graphics, which may alter content. The journal's standard Terms & Conditions and the Ethical guidelines still apply. In no event shall the Royal Society of Chemistry be held responsible for any errors or omissions in this *Accepted Manuscript* or any consequences arising from the use of any information it contains.

ROYAL SOCIETY OF CHEMISTRY

www.rsc.org/obc

View Article Online
DOI: 10.1039/C6OB00681G

Journal Name

ARTICLE

# Synthesis and self-assembly of DNA-chromophore hybrid amphiphiles

Received 00th January 20xx,
Accepted 00th January 20xx

DOI: 10.1039/x0xx00000x

www.rsc.org/

Shine K. Albert, Murali Golla, Hari Veera Prasad Thelu, Nithiyanandan Krishnan, Perapaka Deepak, and Reji Varghese*

DNA based spherical nanostructures is one of the promising nanostructures for several biomedical and biotechnological applications due to their excellent biocompatibility and DNA-directed surface addressability. Herein, we report the synthesis and amphiphilicity-driven self-assembly of two classes of DNA (hydrophilic)-chromophore (hydrophobic) hybrid amphiphiles into spherical nanostructures. A solid-phase "click" chemistry based modular approach is demonstrated for the synthesis of DNA-chromophore amphiphiles. Various spectroscopic and microscopic analyses reveal the self-assembly of the amphiphiles into vesicular and micellar assemblies with corona made of hydrophilic DNA and the hydrophobic chromophoric unit as the core of the spherical nanostructures.

## Introduction

Design and synthesis of biocompatible chromophoric assemblies with well-defined morphology and unique optical properties is challenging.[1] Bottom-up self-assembly using non-covalent interactions is an efficient approach for the creation of functional nanostructures.[2] Numerous examples of chromophoric assemblies that exploit hydrogen bonding,[3] π-π stacking,[4] donor-acceptor,[5] host-guest,[6] and metal-ligand[7] interactions are reported. Amphiphilicity-driven self-assembly is an alternative bottom-up approach for the creation of nanostructures, and is particularly attractive because of the inherent self-assembling tendency of amphiphilic systems.[8] Amphiphiles consist of hydrophobic and hydrophilic moieties joined together either covalently or non-covalently, and are capable of spontaneously assembles into diverse nanostructures such as micelles, vesicles, sheets or tubes mainly through hydrophobic interactions. A unique feature of amphiphilicity-driven self-assembly is the morphology tunability of the nanostructures, which is routinely achieved by controlling the volume ratio between hydrophilic and hydrophobic segments. This approach has been successfully applied in many chromophoric systems for the crafting of nanoarchitectures with interesting optical and electronic properties.[9]

The characteristic structural features of DNA such as predictable secondary structure, nanoscale dimension, ease of synthesis and molecular recognition properties have greatly attracted researchers to use DNA as a building block in the design of DNA based nanostructures. This gave birth to the emerging field of DNA nanotechnology.[10,11] Furthermore, DNA has proven to be an ideal structural scaffold for the helical organization of chromophores either covalently or non-covalently.[12] Very recently, DNA has also been applied as the hydrophilic segment in the design of DNA based amphiphilic systems.[13] The most attractive feature of the self-assembly of DNA based amphiphiles in aqueous medium is the formation of nanostructures with corona made of hydrophilic DNA. Hence, such nanostructures potentially allow the reversible integration of other functional molecules onto their surface through the sequence specific DNA hybridization, which has been exploited for many technological and biomedical applications.[14-20]

The replacement of flexible polymeric segment of conventional DNA amphiphile with a rigid π-conjugated chromophore for the design of DNA amphiphiles has several advantages when compared with the conventional DNA amphiphiles. These include: (i) self-assembly propensity of the amphiphiles is greatly enhanced through the strong π-π-stacking interaction of the chromophoric moiety; (ii) this would also helps in effective encapsulation of the hydrophobic guest molecule through the strong π-stacking as well as hydrophobic interaction of the guest molecules with the chromophoric segment; and (iii) chromophoric rigid block could potentially serve as an optical reporter owing to the modulation of their optical properties upon assembly/disassembly process. However, covalent ligation of hydrophilic DNA and hydrophobic segment is always challenging.[21] The rapid emergence of Cu(I)-catalyzed alkyne-azide cycloaddition (CuAAC) reaction, commonly known as the "click" reaction, have shown ample opportunities in covalent modification of DNA with other functional molecules.[22] Very recently, we have reported a solid-phase "click" chemistry approach for the synthesis of a series of DNA–rigid π-conjugated chromophoric amphiphiles and showed their reversible self-assembly into DNA based surface-engineered vesicles with enhanced emission.[23] Furthermore, we have demonstrated that the DNA-directed surface addressability of the vesicles can be used for the reversible organization of Au-NPs and other fluorophores onto the surface of the vesicle through DNA hybridization. Herein, we report the solid-phase "click chemistry" approach for the synthesis

*School of Chemistry, Indian Institute of Science Education and Research-Thiruvananthapuram (IISER-TVM), CET campus, Trivandrum-695016 (India)*
*E-mail: reji@iisertvm.ac.in*
Electronic Supplementary Information (ESI) available: See DOI: 10.1039/x0xx00000x

This journal is © The Royal Society of Chemistry 20xx



Published on 23 May 2016. Downloaded by University College London on 24/05/2016 16:41:21.

Organic & Biomolecular Chemistry Accepted Manuscript

Please do not adjust margins

View Article Online
DOI: 10.1039/C6OB00681G


Published on 23 May 2016. Downloaded by University College London on 24/05/2016 16:41:21.

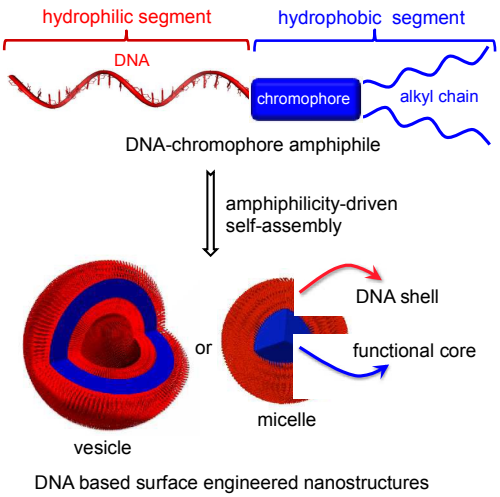


**Fig. 1** Schematic representation depicting the self-assembly of DNA-chromophore hybrid amphiphiles into DNA based surface engineered micelle or vesicle.

of two classes of DNA amphiphiles, DNA-porphyrin (**DNA1**) and DNA-merocyanine (**DNA2**) based systems. These chromophores were chosen in our study due to their promising optical properties and potential applications in various fields.[24] We also report the amphiphilicity-driven self-assembly of DNA-chromophore amphiphiles into vesicular and micellar nanostructures (Fig. 1).

## Results and discussion

### Synthesis of DNA-chromophore amphiphiles

For the synthesis of DNA-chromophore amphiphiles, we adopted a solid phase CuAAC as reported recently by us.[23] For this purpose, alkyne moiety was attached to the 5'-end of a random DNA (3'-ATGTCGATATGAACTTGC-5') using the commercially available C8-alkyne-dT-CE phosphoramidite (**X**) following standard protocols. The CPG bound alkyne functionalized DNA (3'-ATGTCGATATGAACTTGC**X**-5') thus obtained was directly used for the solid phase "click" reaction without further purification. On the other hand, azide modified hydrophobic chromophoric derivatives **3** and **10** were synthesized in multistep synthesis as shown in Scheme 1a. Necessary hydrophobicity to the chromophoric segments was achieved by attaching long hydrocarbon chains ($-C_{18}H_{37}$ or $-C_{12}H_{25}$) to the chromophoric backbone. For the synthesis of azide functionalized porphyrin derivative **3**, bis(octadecyloxy) substituted ester derivative of porphyrin **1** was synthesized from commercially available starting materials.[25] Lithium aluminium hydride ($LiAlH_4$) reduction of the ester **1** followed by the treatment of the corresponding alcohol **2** with 1,8-Diazabicyclo[5.4.0]undec-7-ene (DBU) and diphenylphosphoryl azide (DPPA) furnished the azide functionalized porphyrin derivative **3**. Synthesis of azide modified merocyanine derivative **10** was started from the commercially available N-(3,5-dihydroxyphenyl)acetamide, which was converted into 3,5-bis(dodecyloxy)aniline (**4**) through multi step synthesis following a reported procedure.[26] Reaction between **4** and cyanoacetic acid (**5**) in the presence of N,N'-dicyclohexylcarbodiimide (DCC) gave the bis(dodecyloxy) amide derivative **6**, which upon condensation with ethyl acetoacetate (**7**) furnished the hydroxypyridone derivative **8**. Subsequent treatment of **8** with N,N-diphenylformamidine (DPFA) in acetic anhydride afforded the corresponding enaminone derivative, which was treated in-situ with the azide functionalized pyridinium salt **9** in the presence of potassium acetate (KOAc) as base furnished the azide modified merocyanine derivative **10**. Synthesis of DNA-chromophore amphiphiles (**DNA1** and **DNA2**) was achieved by the solid-phase "click" reaction between the CPG bound 5'-alkyne modified DNA (3'-ATGTCGATATGAACTTGC**X**-5') and the corresponding azide functionalized chromophore derivative (**3** or **10**) in a mixture of DMSO and t-BuOH (3:1) in the presence of Cu(I)Br as catalyst with tris[(1-benzyl-1H-1,2,3-triazol-4-yl)methyl]amine (TBTA) as the ligand at 60 °C for 24 h. Subsequently, the DNA was deprotected from the solid support using ammonium hydroxide solution (28 %) provided the DNA-chromophore amphiphiles **DNA1** and **DNA2**, which was subsequently purified and characterized through ESI-MS analysis (Scheme 1b).

### Optical Studies

Self-assembly of the amphiphiles **DNA1** and **DNA2** was performed by heating the respective amphiphile (1 μM) in Tris buffer (50 mM, pH 7.4) at 90 °C for 5 min and then allowing to cool to room temperature. UV-Vis absorption spectra of **DNA1** and **DNA2** show the characteristic absorption of DNA and the corresponding chromophoric segments. Temperature-dependent UV-Vis absorption spectra of **DNA1** and **DNA2** provided better understanding into the self-assembly of these amphiphiles. Absorption spectrum of **DNA1** shows the characteristic absorption peaks of aggregated porphyrin at 418 nm (Soret-band) and 549 nm (Q-band).[27] Temperature dependent absorption spectrum of **DNA1** shows only a slight decrease in the absorption bands at 418 nm and 549 nm with no change in the absorption maximum (Fig. 2a). Similarly, absorption spectrum of **DNA2** shows the characteristic absorption of merocyanine and DNA at 480 nm and 260 nm, respectively (Fig. 2b).[28] In this case, temperature dependent absorption spectrum shows a gradual red-shift of 7 nm in the absorption maximum of merocyanine from 480 nm to 487 nm with the increase in temperature from 20 °C to 70 °C. In accordance with this, the temperature dependent excitation spectrum also shows a red-shift of 7 nm with the increase in the temperature (Fig. 2b inset). Furthermore, **DNA1** and **DNA2** aggregates display induced circular dichroism (ICD) signals in the absorption regions of the respective chromophores, indicating the transfer of molecular chirality of DNA to the chromophoric stacks of the aggregates of **DNA1** and **DNA2** (Figure 2c, d). No change is observed in the intensity of the ICD signals of **DNA1** and **DNA2** aggregates with the increase in temperature. Fluorescence spectrum of **DNA1** displays the characteristic emission of self-assembled porphyrin with maximum centered at 645 nm ($\lambda_{ex}$ = 420 nm). The quantum yield of **DNA1** is 0.01. Notably, no significant change, except a slight decrease in the emission intensity is observed in the temperature-dependent fluorescence spectrum of **DNA1** (Fig. 3a), which is in accordance with the temperature dependent absorption spectral studies. Emission spectrum of **DNA2** shows the characteristic emission of aggregated merocyanine at 698 nm ($\lambda_{ex}$ = 480 nm), which also shows a gradual decrease in emission intensity upon increasing the temperature from 20 °C to 80 °C (Fig. 3b). In order to understand whether the observed photophysical changes of **DNA1** and **DNA2** aggregates with temperature is indeed due to the disassembly of

Organic & Biomolecular Chemistry Accepted Manuscript


This journal is © The Royal Society of Chemistry 20xx

Please do not adjust margins

View Article Online
DOI: 10.1039/C6OB00681G



Published on 23 May 2016. Downloaded by University College London on 24/05/2016 16:41:21.

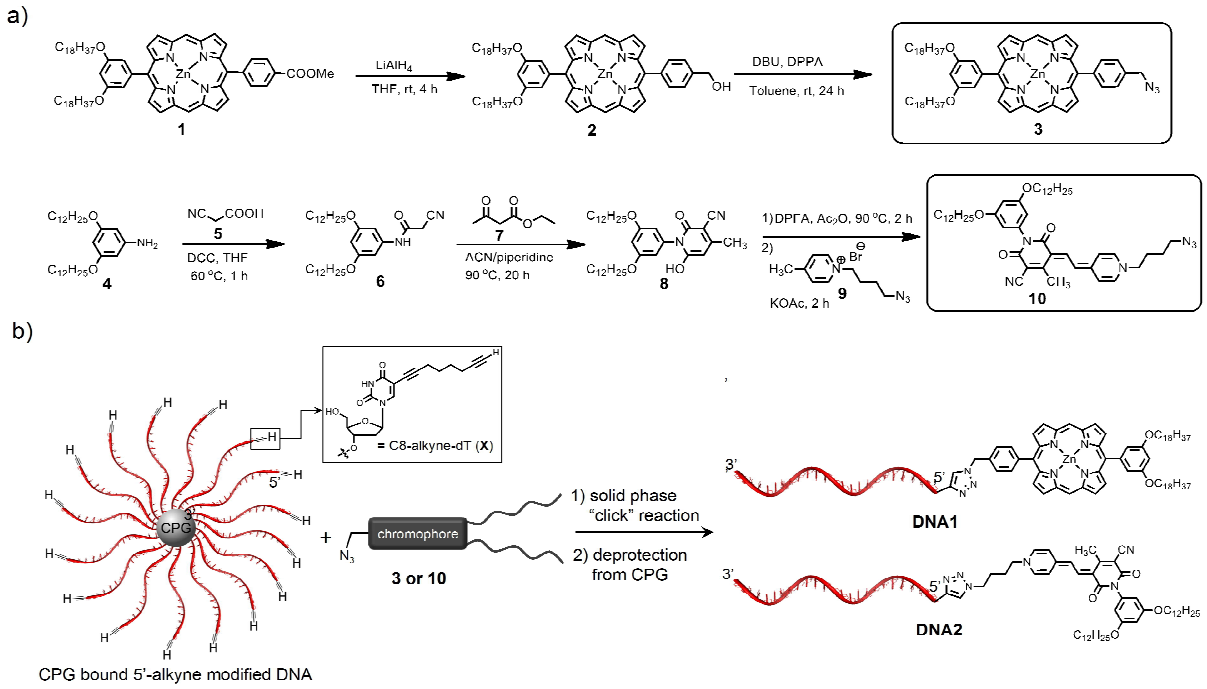


**Scheme 1**. (a) Synthetic scheme for azide functionalized chromophores **3** and **10**. (b) Synthesis of DNA-chromophore amphiphiles (**DNA1** and **DNA2**) through solid-phase CuAAC reaction between CPG bound 5'-alkyne modified DNA (3'-ATGTCGATATGAACTTGC**X**-5') and azide functionalized chromophores (**3** or **10**).

the aggregates, as expected or the mere effect of temperature on photophysical properties, variable temperature optical studies were carried out on **3** and **10**. Azide derivatives **3** and **10** are the precursor chromophores for **DNA1** and **DNA2**, respectively. The effect of temperature on the photophysical properties of these chromophores was studied by doing variable temperature optical studies of the monomeric species of **3** and **10**. Experiments were performed in chloroform as the solvent, where the precursor chromophores **3** and **10** exist as monomeric species. Interestingly, temperature-dependent absorption and emission studies of **3** and **10** revealed similar photophysical changes as that of **DNA1** and **DNA2** aggregates, respectively (Fig. S1-4). These observations suggest that the observed photophysical changes for **DNA1** and **DNA2** aggregates with temperature could be the mere effect of temperature on the photophysical properties of **DNA1** and **DNA2** aggregates, and not due to the temperature induced disassociation of the aggregates.

**Dynamic Light Scattering (DLS) Studies**

To get more insight into the morphology of the aggregated species of **DNA1** and **DNA2** in solution, detailed DLS analyses were carried out. The DLS analyses of **DNA1** and **DNA2** show the formation of equilibrated nanometer sized spherical particles in solution. The micellar or vesicular nature of the spherical particles observed in DLS can easily be distinguished by comparing the experimental particle size and the calculated bilayer packing distance, which is equal to twice the molecular length of the amphiphile. It is to be noted that in our case, interdigitation of alkyl chains and a helical conformation for ssDNA segment of DNAs were assumed as shown in Fig. 7 for the calculation of bilayer distance for **DNA1** and **DNA2**. Accordingly, the calculated bilayer distances for **DNA1** and **DNA2** are ~22 nm, ~21 nm, respectively. For the micellar assemblies the particle size would be equal to the bilayer packing distance, whereas, in the case of vesicular assemblies the particle size would be significantly larger than the bilayer packing distance, because bilayer distance in the case of vesicles represents only the wall thickness of the vesicles.[29] The DLS analysis of **DNA1** at 20 °C shows unimodal distribution of spherical particles with size ranging from 120 nm to 530 nm (σ = 0.296) with an average diameter of 272 nm (Fig. 4a). The diameter of the smallest particle (120 nm) is considerably larger than the calculated bilayer distance of **DNA1** (~22 nm), clearly revealing the vesicular nature for **DNA1** particles. Interestingly, DLS analysis at 70 °C reveals that vesicles are not dissociating into the monomers even at high temperature (Fig. 4a). This is in accordance with the temperature dependent optical studies of **DNA1**, and confirms that the vesicles are thermally stable, at least up to 70 °C. On the other hand, a narrow unimodal distribution of spherical aggregates with particle size ranging from 25 nm to 95 nm (σ = 0.273) with an average diameter of 47 nm is observed for **DNA2** aggregates (Fig. 4b). In this case, it is important to note that the smallest particle has a diameter of 25 nm, which is approximately equal to the calculated bilayer distance of **DNA2** (~21 nm). This clearly implies that the spherical aggregates of **DNA2** are micellar in nature, and not vesicular. The larger spherical particles (>25 nm) observed for **DNA2** assemblies could be the aggregated micelles in solution. In this case also, in accordance with the temperature dependent optical studies, DLS analysis at 70 °C

Organic & Biomolecular Chemistry Accepted Manuscript



Please do not adjust margins

View Article Online
DOI: 10.1039/C6OB00681G


Published on 23 May 2016. Downloaded by University College London on 24/05/2016 16:41:21.

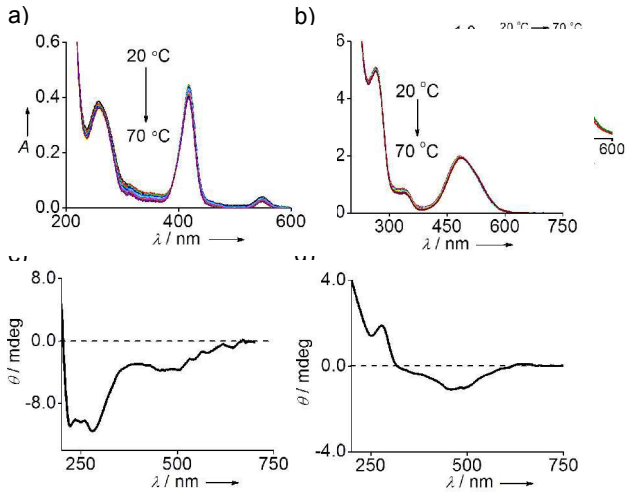


**Fig. 2** Temperature dependent absorption spectra of (a) **DNA1** and (b) **DNA2**. Inset shows variable temperature excitation spectrum (normalized) of **DNA2** (monitored at $\lambda_{em}$ = 698 nm). CD spectra of (c) **DNA1** and (d) **DNA2** at 20 °C. All experiments were performed with 1 µM DNA in 50 mM Tris buffer, pH 7.4, path length of the cell = 10 mm.

shows that micelles are thermally stable, and hence not dissociating into the corresponding monomers with the increase in temperature (Fig. 4b). These results clearly suggest that the amphiphiles **DNA1** and **DNA2** undergoes amphiphilicity-driven self-assembly in aqueous medium into thermally stable vesicles and micelles, respectively. Furthermore, zeta potential measurements respectively show –4.58 mV, and –4.46 mV values for **DNA1** and **DNA2** (Fig. S7), indicating the negatively charged surfaces of **DNA1** vesicle and **DNA2** micelle as expected.

**Dye Encapsulation and Microscopic Studies**

Better insights into the morphology of these aggregates were provided by the dye encapsulation and microscopic studies. Clear evidence for the vesicular nature for the spherical aggregates of **DNA1** was obtained from the encapsulation studies with Calcein. Calcein is a fluorescent hydrophilic dye, and hence would be encapsulated in the hydrophilic interior of the vesicle.[30] A significant quenching is observed for the emission intensity of Calcein encapsulated inside the **DNA1** vesicle when compared with the emission of an absorption matched solution of Calcein in vesicle-free solution ($\lambda_{ex}$ = 470 nm, Fig. 5a). This can be attributed to the self-quenching of the dye emission due to the high encapsulation of Calcein in the hydrophilic cavity of **DNA1** vesicle. Laser Scanning Confocal Microscope (LSCM), Atomic Force Microscope (AFM), and Transmission Electron Microscope (TEM) were also used to study the self-assembled nanostructures of **DNA1** and **DNA2** amphiphiles. In accordance with the fluorescence properties of **DNA1**, LSCM images show the formation of fluorescent vesicles for **DNA1** ($\lambda_{ex}$ = 405 nm, Fig. 5b). The height images of self-assemblies of **DNA1** obtained by tapping-mode AFM show the formation of nanometer sized spherical assemblies (Fig. 6a). The average diameter of the spheres of **DNA1** assemblies, which were estimated from the fitted histograms of the size distribution curves after subtracting the tip-broadening factor, is ~250 nm. This is in good agreement with the

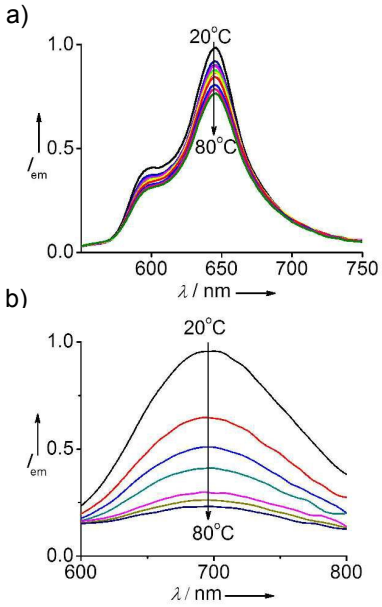


**Fig. 3** Normalized temperature dependent emission spectra of (a) **DNA1** ($\lambda_{ex}$ = 420 nm) and (b) **DNA2** ($\lambda_{ex}$ = 480 nm). All experiments were performed with 1 µM DNA in 50 mM Tris buffer, pH 7.4, path length of the cell = 10 mm.

average diameter of the particles obtained from DLS analysis. The cross-sectional analysis of the vesicles reveals that the average height of the vesicle is only ~11 nm, much smaller than their respective average diameter. The low average height of **DNA1** vesicles can be attributed to the considerable flattening of the vesicles on the mica surface, which is a characteristic feature of

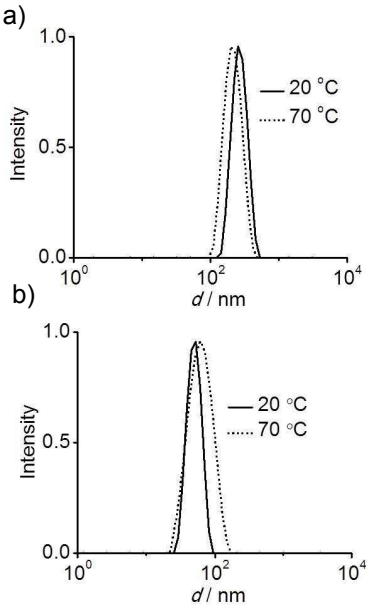


**Fig. 4** Size distribution graphs from the DLS measurements of (a) **DNA1**, and (b) **DNA2** at 20 °C (solid line) and 70 °C (dotted line). All experiments were performed with 1 µM DNA in 50 mM Tris buffer, pH 7.4.

Organic & Biomolecular Chemistry Accepted Manuscript


This journal is © The Royal Society of Chemistry 20xx

Please do not adjust margins

View Article Online
DOI: 10.1039/C6OB00681G



Published on 23 May 2016. Downloaded by University College London on 24/05/2016 16:41:21.

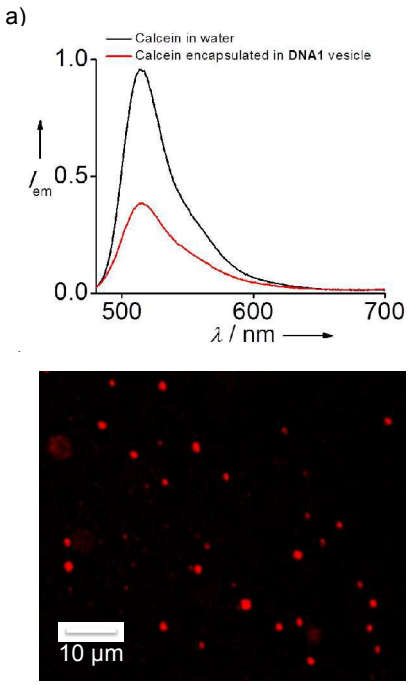


**Fig. 5** (a) Fluorescence spectra of Calcein encapsulated in **DNA1** vesicle and Calcein in vesicle-free solution ($\lambda_{ex}$ = 470 nm). (b) LSCM image of **DNA1** vesicle ($\lambda_{ex}$ = 405 nm).

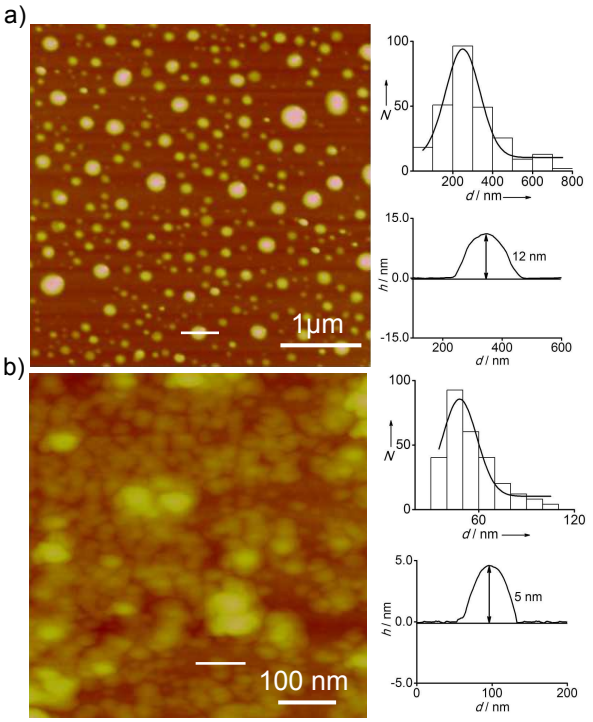


**Fig. 6** AFM height images of (a) **DNA1** (z-scale = 25 nm) and (b) **DNA2** (z-scale = 50 nm) with the corresponding the particle size distributions. A representative cross-section analysis of a single particle is also shown. All experiments were performed on a freshly cleaved mica surface.

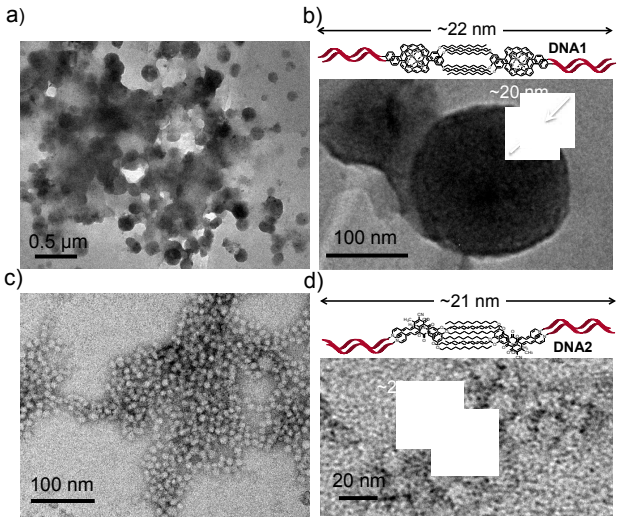


**Fig. 7** Zoom-out TEM images of (a) **DNA1** and (c) **DNA2**, and the corresponding zoom-in TEM images of (b) **DNA1** and (d) **DNA2** on a carbon coated grid. Schematic representations of the proposed bilayer packing of the amphiphiles are also shown.

"soft" vesicles.[31] On the other hand, AFM analysis of **DNA2** assemblies shows the formation of spherical particles with size ranging from ~20 nm to ~90 nm (Fig. 6b). The average height of the particle is ~7 nm as revealed from the cross-sectional analysis. The micellar nature of **DNA2** assemblies is clear from the approximate matching of the diameter of the smallest particle (~20 nm) with the calculated bilayer packing distance for **DNA2** (~21 nm). The morphology of the spherical aggregates of **DNA1** and **DNA2** deduced from various spectroscopic and microscopic studies were unequivocally confirmed by the TEM analyses of the nanostructures. For **DNA1**, spherical particles of diameters in the range of 100–400 nm with clear contrast difference between the periphery and the inner part of the spheres are observed in the TEM analysis (Fig. 7a, b), which is a conclusive evidence for the vesicular nature for the spheres of **DNA1**. More importantly, the wall thickness of the vesicle calculated from the TEM images (~20 nm) is approximately equal to the calculated wall thickness (~22 nm). However, 2 nm decrease in the experimentally observed wall thickness compared with the calculated value can be attributed to the flexible nature of the alkyl chains, the linker, and the ssDNA segments of **DNA1**. On the other hand, TEM images of **DNA2** aggregates show the formation of spherical particles with almost uniform size of ~20 nm, which is approximately equal to the bilayer packing distance for **DNA2** (~21 nm, Fig. 7c, d). This confirms that the spherical aggregates of **DNA2** are micellar in nature as revealed by other spectroscopic and microscopic techniques. It is worth noting that no change is observed in vesicular morphology of **DNA1** and micellar morphology of **DNA2** even after hybridization of ssDNA on their surface with the corresponding complementary DNA strand (5'-TACAGCTATACTTGAACG-3') (Fig. S8). We have also carried out detailed morphological studies of the aggregates of **3** and **10**, which were obtained by the addition of water into the THF solution of **3** and **10**, in order to compare their self-assembling properties with the corresponding DNA based amphiphiles. Interestingly, fibrous morphology was observed for the aggregates of **3** and **10** from the respective AFM analyses (Fig. S9 and S10). Optical and

Organic & Biomolecular Chemistry Accepted Manuscript



Please do not adjust margins

View Article Online
DOI: 10.1039/C6OB00681G


Published on 23 May 2016. Downloaded by University College London on 24/05/2016 16:41:21.

morphological studies clearly reveal that aggregates of **3** and **10** and the corresponding amphiphiles (**DNA1** and **DNA2**) exhibit dissimilar optical and morphological properties, and hence it can be concluded that DNA induced amphiphilicity-driven self-assembly leads to unique functional nanostructures.

## Conclusions

In summary, we have reported a solid-phase "click" chemistry based modular approach for the synthesis of DNA (hydrophilic)-chromophore (hydrophobic) hybrid amphiphiles, and demonstrated their amphiphilicity driven self-assembly into DNA based surface engineered spherical nanostructures. The generality of the synthetic approach was demonstrated through the synthesis of two different classes of DNA-chromophore amphiphiles. Temperature-dependent optical and light scattering analyses have revealed that the amphiphiles are self-assembling into thermally stable spherical nanostructures. Detailed microscopic analyses have shown that the **DNA1** self-assemble into vesicular nanostructures, whereas **DNA2** self-assemble into micellar nanostructures. One of the most striking features of this class of nanostructures is the dense display of DNA their surface, which makes this kind of nanostructures biocompatible and surface addressable, and hence would be an ideal candidate for diverse biomedical and biotechnological applications. We hope the "click" chemistry based modular synthesis and unique structural features of this kind nanostructures may encourage researchers to design other classes of DNA-chromophores hybrid amphiphiles for addressing the challenges in drug delivery and nanoelectronics.

## Experimental

Compounds **1**,[25] and **4**[26] were obtained through multistep synthesis as per the reported procedures. All chemicals used for the organic synthesis were purchased from Sigma Aldrich and were used as received. Solvents were dried using the standard procedures wherever required. Column chromatography was done on 200-400 mesh silica gel. TLC analyses were performed on aluminium plates coated with silica gel 60 F254. Melting points were recorded on SMP30 melting point apparatus and are uncorrected. $^{1}$H and $^{13}$C spectra were recorded on Bruker Avance-III 500 MHz NMR Spectrometer. Deuterated solvents containing 1,1,1,1-tetramethylsilane as internal standard was used for recording NMR. Shimadzu IR prestige-21 FT-IR was used for recording IR spectra where solid samples were pelletized along with KBr. Water used for all the experiments was de-ionised Milli Q (18.2 MΩ.cm). All phosphoramidites for the oligonucleotide synthesis were purchased from Glen Research and were used as received. Alkyne modified oligonucleotides were synthesized on H-8 K&A DNA/RNA synthesizer in 1 µmole scale. AFM imaging was done on Multimode SPM (Veeco Nanoscope V). Samples were prepared by depositing 2 µL of aggregated samples on freshly cleaved mica surface and were dried under air. Images were recorded under ambient conditions in tapping mode. Probe used for imaging was antimony doped silicon cantilever with a resonant frequency of 300 kHz and spring constant of 40 Nm$^{-1}$. TEM analyses were carried out on FEI Tecnai 30 G2 (300 kV) High Resolution-TEM. Sample preparation was done by drop-casting 2 µL of sample on negatively glow discharged (PELCO easiGlow) 400-mesh carbon coated copper grid (Ted Pella, Inc.). Samples were allowed to adsorb on grid for 2 min and excess sample was wicked with filter paper. Grid was washed twice by touching grid with a drop of water and then removing excess water using filter paper and was stained with 0.7% uranyl formate solution. Absorption spectra were recorded on a peltier attached Shimadzu UV-3600 Vis-NIR Spectrophotometer in a quartz cuvette of 10 mm path length. Steady state fluorescence and excitation spectra were recorded on a Horiba Jobin Vyon Fluorimeter equipped with peltier cell holder. Temperature dependent emission experiments were carried out by heating samples from 20 °C to 70 °C at an interval of 5 °C equilibrating samples for 5 minutes at each temperature before recording the spectra and were given correction for solvents. DLS analyses were done on Malvern Zetasizer Nano Zs equipped with 655 nm laser. Experiments were performed at 25 °C at a back scattering angle of 173°. HR-MS analysis was done on thermo extractive orbitrap mass spectrometry. ESI-MS was recorded on Waters Xevo G2 QTof and GC-MS on Shimadzu GCMS-QP2010. Confocal microscopic analysis was done on inverted Leica SP5-DMRX Laser Confocal Microscope. Sample was prepared by drop casting the solution on a cleaned glass slide and was dried under vacuum. ProLong Gold (antifade reagent) was used to mount the cover slip and imaging was done in 63X magnification in presence of immersion oil.

**Synthesis of 2**: To a solution of **1** (0.100 g, 0.0892 mmol) in freshly distilled THF (2 mL), $LiAlH_4$ (2M, 6 mL) was added and stirred at 0 °C for 1 h. Then the temperature was slowly increased to room temperature and was stirred 4 h. After completion of the reaction, reaction mixture was poured into ice-cold water and was extracted with ethyl acetate. Organic layer was dried over anhydrous $Na_2SO_4$ and the solvent was removed. The crude product was purified using column chromatography using petroleum ether:ethyl acetate (80:20) as eluent to get desired product as dark purple solid (90%). M.P. 76 °C; TLC (petroleum ether:ethyl acetate, 80:20) $R_f$ = 0.27; $^{1}$H NMR (500 MHz, $CDCl_3$), δ (ppm) = 0.78 (t, J = 7.1 Hz, 6H), 1.14–1.20 (m, 52H), 1.25–1.29 (m, 4H), 1.40–1.44 (m, 4H), 1.50–1.80 (m, 4H), 1.77–1.80 (m, 4H), 4.06 (t, J = 5 Hz, 4H), 4.74 (s, 2H), 6.83 (t, J = 2.3 Hz, 1H), 7.35 (d, J = 2.2 Hz, 2H), 7.55 (d, J = 7.7 Hz, 2H), 8.12 (d, J = 7.7 Hz, 2H), 9.01 (d, J = 4.35 Hz, 2H), 9.18 (d, J = 4.45 Hz, 2H), 9.32–9.34 (m, 4H), 10.20 (s, 2H); $^{13}$C NMR (125 MHz, $CDCl_3$), δ (ppm) = 14.11, 22.68, 26.14, 29.35, 29.43, 29.46, 29.61, 29.64, 29.68, 31.92, 65.25, 68.44, 100.97, 106.18, 114.55, 119.23, 120.30, 125.19, 131.69, 131.72, 132.36, 132.66, 133.71, 134.77, 142.06, 144.36, 149.44, 149.59, 149.99, 150.03, 158.35. HR-MS (m/z); $[M+H]^+$ calcd. for $[C_{69}H_{95}N_4O_3Zn]^+$: 1091.6617; found: 1091.6668.

**Synthesis of 3**: To a solution of **2** (0.057 g, 0.05 mmol) in freshly dried toluene (2 mL), 1,8-diazabicyclo[5.4.0]undec-7-ene (DBU) (10 µL, 0.07 mmol) and diphenylphosphoryl azide (DPPA) (13.5 µL, 0.06 mmol) were added and the reaction mixture was stirred at room temperature for 24 h. After completion of the reaction saturated $NH_4Cl$ was added and was extracted with ethyl acetate. Organic layer was dried over anhydrous $Na_2SO_4$ and solvent was removed. Crude product was further purified using column chromatography using petroleum ether:ethyl acetate (80:20) as eluent to get the desired product as dark purple solid (90%). M.P. 70 °C; TLC (petroleum ether:ethyl acetate) $R_f$ = 0.6; IR (KBr): 2927, 2854, 2100, 1597, 1259, 1097, 920, 763 cm$^{-1}$. $^{1}$H NMR (500 MHz, $CDCl_3$), δ (ppm) = 0.77 (t, J = 7.0 Hz, 6H), 1.14–1.21 (m, 52H), 1.28–1.32 (m, 6H), 1.38–1.40 (m, 4H), 1.42–1.43 (m, 4H), 1.79–1.83 (m, 4H), 4.08 (t, J = 2.4 Hz, 4H), 4.61 (s, 2H), 6.84 (t, J = 2.0 Hz, 1H), 7.35 (d, J = 2.5 Hz, 2H), 7.44 (d, J = 6.4 Hz, 2H), 8.16 (d, J = 8.0 Hz, 2H), 8.99 (d, J = 4.50 Hz, 2H), 9.18 (d, J = 4.50 Hz, 2H), 9.36 (t, J = 4.0 Hz, 4H), 10.24 (s, 2H); $^{13}$C NMR (125 MHz, $CDCl_3$), δ (ppm) = 14.06, 22.65, 26.13,

Organic & Biomolecular Chemistry Accepted Manuscript


This journal is © The Royal Society of Chemistry 20xx

Please do not adjust margins

View Article Online
DOI: 10.1039/C6OB00681G


Published on 23 May 2016. Downloaded by University College London on 24/05/2016 16:41:21.

29.31, 29.45, 29.59, 29.60, 29.64, 31.89, 54.85, 68.44, 101.01, 106.25, 114.55, 119.19, 120.14, 126.43, 131.75, 131.79, 132.25, 132.71, 134.58, 134.93, 142.76, 144.27, 149.47, 149.64, 149.88, 150.07, 158.37. HR-MS (m/z); $[M+H]^+$ calcd. for $[C_{67}H_{94}N_7O_2Zn]^+$: 1116.6682; found: 1116.6728.

**Synthesis of 6**: A solution of **4** (5 g, 10.84 mmol) and cyanoacetic acid (1.19 g, 14.09 mmol) in freshly dried and distilled THF was stirred at 70 °C for 1 h and DCC (2.90 g, 14.09 mmol) was added to the hot reaction mixture. It was then cooled to room temperature, solvent was removed and crude product was purified by column chromatography using dichloromethane as eluent to get desired product as white solid (75%). M.P. 62.0 °C; TLC (dichloromethane) $R_f$ = 0.37; $^1$H NMR (500 MHz, $CDCl_3$) δ (ppm) = 0.80 (t, J = 7 Hz, 6H), 1.19–1.25 (m, 34H), 1.32–1.36 (m, 4H), 1.60–1.70 (m, 4H), 3.44 (s, 2H), 3.83 (t, J = 6.5 Hz, 4H), 6.20 (s, 1H), 6.60 (d, J = 1.9, 2H), 7.55 (s, 1H); $^{13}$C NMR (125 MHz, $CDCl_3$) δ (ppm) = 14.09, 22.67, 24.65, 25.20, 26.01, 29.33, 29.60, 30.83, 31.90, 32.35, 40.84, 50.61, 68.19, 98.37, 99.05, 114.66, 138.58, 152.76, 159.48, 160.57. HR-MS (m/z); $[M+H]^+$ calcd. for $[C_{33}H_{57}N_2O_3]^+$: 529.4291; found: 529.4359.

**Synthesis of 8**: To a solution of **6** (1.0 g, 1.89 mmol) and ethylacetocetate (0.254 g, 1.89 mmol) in acetonitrile (5 mL), piperidine (0.46 mL) was added and heated at 90 °C for 20 h. After the reaction, solvent was removed and crude product was filtered on silica neutralized with triethylamine using dichloromethane as eluent to get desired product as dark brown semi solid (43%). TLC (dichloromethane) $R_f$ = 0.31; $^1$H NMR (500 MHz, $CDCl_3$) δ (ppm) = 0.80 (t, J = 7 Hz, 6H), 1.06–1.32 (m, 34H), 1.62–1.66 (m, 4H), 2.13 (s, 3H), 3.80 (s, 4H), 5.50 (s, 1H), 6.22(s, 2H), 6.33 (s, 1H), 10.48 (s, 1H); $^{13}$C NMR (125 MHz, DMSO-$d_6$) δ (ppm) = 8.66, 13.89, 20.38, 22.05, 25.48, 28.61, 28.66, 28.69, 28.94, 28.97, 28.99, 31.26, 45.79, 54.82, 67.48, 75.58, 98.83, 99.60, 108.12, 121.56, 140.45, 151.98, 159.45, 163.76, 164.25. HR-MS (m/z); $[M+H]^+$ calcd. for $[C_{37}H_{59}N_2O_4]^+$: 595.4397; found: 595.4818.

**Synthesis of 10**: A solution of **8** (0.4g, 0.67 mmol) and N,N'-diphenylformamidine (0.67 mmol) in acetic anhydride (0.67 mL) was stirred (~15 min) at room temperature till the reaction mixture become solid and was then stirred at 90 °C for 15 min and cooled to room temperature. To this reaction mixture **9** (0.15 g, 0.67 mmol) and potassium acetate (0.06 g, 0.67 mmol) was added and stirred at 90 °C for 2 h. After reaction acetic anhydride was removed under reduced pressure and the product was purified by column chromatography using dichloromethane:methanol as eluent (98:2) to get desired product as dark brown solid (67%). M.P. 174.0 °C; TLC (dichloromethane) $R_f$ = 0.37; IR (KBr): 3057, 2922, 2852, 2193, 2094, 1658, 1593, 1564, 1490, 1390, 1282, 1161, 833, 744 $cm^{-1}$. $^1$H NMR (500 MHz, $CD_2Cl_2$), δ (ppm) = 0.81 (t, J = 7 Hz, 6H), 1.18–1.45 (m, 43H), 1.50–1.52 (m, 2H), 1.64–1.68 (m, 4H), 1.85–1.90 (m, 2H), 2.44 (s, 3H), 3.31 (t, J = 6.5 Hz, 2H), 3.83 (t, J = 6.5 Hz, 4H), 4.01 (t, J = 4 Hz, 2H), 6.19 (s, 2H), 6.37 (t, J = 2 Hz, 1H), 7.30 (d, J = 6.5 Hz, 2H), 7.58 (d, J = 7.5 Hz, 2H), 7.71 (d, J = 2 Hz, 2H); $^{13}$C NMR (125 MHz, $CD_2Cl_2$) δ (ppm) = 13.89, 18.70, 22.69, 25.48, 26.04, 28.34, 29.27, 29.35, 29.43, 29.62, 29.64, 29.65, 29.68, 31.92, 50.74, 58.72, 68.29, 87.91, 100.59, 106.33, 107.55, 113.80, 119.32, 120.51, 139.35, 139.53, 140.60, 156.86, 156.99, 160.58, 163.20, 163.53. HR-MS (m/z); $[M+H]^+$ calcd. for $[C_{48}H_{71}N_6O_4]^+$: 795.5459; found: 795.5530.

**General procedure for the synthesis of DNA1 and DNA2**: Azide modified chromophore derivative (**3** or **10**, 20 µmol) was dissolved in 200 µL of dry THF in a glass vial. Cu(1)Br (1.5 mg, 10 µmol) was dissolved in 100 µL of freshly prepared DMSO:t-butanol (3:1) mixture. Tris[(1-benzyl-1H-1,2,3-triazol-4-yl)methyl]amine (TBTA, 5.3 mg, 10 µmol) was dissolved in 50 µL of DMSO:t-butanol (3:1) mixture. Subsequently, solution of **3** or **10** (200 µL) was added to the solution of Cu(1)Br (100 µL) and TBTA (50 µL) in a 5 mL two-neck glass flask. The mixture was degassed by three cycles of freeze-pump-thaw method. CPG bound alkyne modified DNA (1 µmol) was added to the degassed solution under argon purging and stirred at 60 °C for 24 h. Afterward, the beads were washed repeatedly with THF, DCM and finally with acetonitrile for several times (minimum 10 times) and then dried under vacuum. Beads were transferred into a 2 mL Eppendorf vials, 1 mL of 28 % ammonia solution was added and vortexed for 24 h at room temperature. Beads were removed by filtering using centrifugal filters (0.45 µm filter size, Millipore Ultrafree MC). After removing the ammonia using speed vacuum, sodium acetate solution (0.3 M, 100 µL) was added to this and was again vortexed at room temperature for another 1 h. Solution was then filtered using centrifugal filter (0.45 µm filter size, Millipore Ultrafree MC). Unconjugated DNAs were then removed through Amicon centrifugal filters. Purification was done by centrifuging the DNA solution 5 times at 8800 rpm for 3 minutes using 3K filters (Milipore UFC50003BK) followed by centrifuging 20 times using 30K filters (Milipore UFC5030BK) at 5000 rpm for 3 minutes. Purity of the DNAs was confirmed by gel electrophoresis analysis (20% denaturing PAGE), and were characterized through ESI-MS analyses. Mass calcd. for **DNA1**: 7002.61; found 7001.98; mass calcd. for **DNA2**: 6681.48; found 6682.37.

**Calcein encapsulation studies:** Stock solution of Calcein was prepared in methanol. Stock solution was taken in a vial and solvent was evaporated. Solution of **DNA1** (1 µM) in water was added into the Calcein solution so that final concentration of Calcein was 0.5 µM. Solution was sonicated for 1 minute and was then heated to 90 $^o$C and was maintained at 90 $^o$C for 5 minutes on a thermal shaker. It was then switched off and solution was allowed to cool to room temperature. Unencapsulated Calcein was removed by using 3 KDa molecular weight cut-off centrifugal filters from Amicon. Filtration was done by centrifuging the sample at 5800 rpm for 3 minutes. Centrifuging was repeated for nearly 20 times and afterwards emission was recorded by exciting the sample at 470 nm. Control experiment was done by dissolving Calcein in water in such a way that concentration of Calcein in control as well as experimental solution was same.

## Acknowledgements

We thank the financial support from DBT (No. BT/PR7030/NNT/28/636/2012). R.V. is grateful to the DST for a Ramanujan Fellowship. S.K.A. thanks CSIR, and H.V.P.T. and N.K. acknowledge UGC for research fellowships. We are thankful to University of Madras for TEM experiments. We acknowledge CSIR-NIIST for HR-MS and M.G. University for ESI-MS analyses.

## Notes and references

1 (a) J.-M. Lehn, *Science*, 2002, **295**, 2400–2403; (b) S. I. Stupp, *Nano Lett.*, 2010, **10**, 4783–4786; (c) T. Aida, E. W. Meijer and S. I. Stupp, *Science*, 2012, **335**, 813–817.

2 (a) L. J. Prins, D. N. Reinhoudt and P. Timmerman, *Angew. Chem., Int. Ed.*, 2001, **40**, 2382–2426; (b) L. Brunsveld, B. J. B. Folmer, E. W. Meijer and R. P. Sijbesma, *Chem. Rev.*, 2001, **101**, 4071–4097; (c) F. Würthner, *Chem. Commun.*, 2004, 1564–1579; (d) A. C. Grimsdale and K. Müllen, *Angew.*

Organic & Biomolecular Chemistry Accepted Manuscript



Please do not adjust margins

View Article Online
DOI: 10.1039/C6OB00681G


*Chem., Int. Ed*., 2005, **44**, 5592–5629; (e) F. J. M. Hoeben, P. Jonkheijm, E. W. Meijer and A. P. H. J. Schenning, *Chem. Rev*., 2005, **105**, 1491–1546; (f) S. S. Babu, V. K. Praveen and A. Ajayaghosh, *Chem. Rev.*, 2014, **114**, 1973–2129.

3 (a) C. Thalacker and F. Würthner, *Adv. Funct. Mater*., 2002, **12**, 209–218; (b) K. Sugiyasu, N. Fujita and S. Shinkai, *Angew. Chem., Int. Ed*., 2004, **43**, 1229–1233; (c) A. Ajayaghosh, R. Varghese, S. J. George and C. Vijayakumar, *Angew. Chem., Int. Ed.*, 2006, **45**, 1141–1144; (d) E.-K. Schillinger, E. Mena-Osteritz, J. Hentschel, H. G. Börner and P. Bäuerle, *Adv. Mater*., 2009, **21**, 1562–1567; (e) S. Yagai, Y. Goto, X. Lin, T. Karatsu, A. Kitamura, D. Kuzuhara, H. Yamada, Y. Kikkawa, A. Saeki and S. Seki, *Angew. Chem., Int. Ed.*, 2012, **51**, 6643–6647.

4 (a) A. Ajayaghosh, R. Varghese, V. K. Praveen and S. Mahesh, *Angew. Chem., Int. Ed*., 2006, **45**, 3261–3264; (b) Y. Tang, Z. Zhou, K. Ogawa, G. P. Lopez, K. S. Schanze and D. G. Whitten, *Langmuir*, 2009, **25**, 21–25; (c) C. Kulkarni and S. J. George, *Chem. Eur. J.*, 2014, **20**, 4537–4541; (d) C. Rest, M. J. Mayoral, K. Fucke, J. Schellheimer, V. Stepanenko and G. Fernández, *Angew. Chem., Int. Ed.*, 2014, **53**, 700–705; (e) R. T. Cheriya, A. R. Mallia and M. Hariharan, *Energy Environ. Sci.*, 2014, **7**, 1661–1669.

5 (a) J. J. Reczek, K. R. Villazor, V. Lynch, T. M. Swager and B. L. Iverson, *J. Am. Chem. Soc*., 2006, **128**, 7995–8002; (b) K. Liu, C. Wang, Z. Li and X. Zhang, *Angew. Chem., Int. Ed*., 2011, **50**, 4952–4956; (c) K. Jalani, M. Kumar and S. J. George, *Chem. Commun*., 2013, **49**, 5174–5176.

6 (a) A. Harada, Y. Takashima and H. Yamaguchi, *Chem. Soc. Rev*., 2009, **38**, 875–882; (b) D. Jiao, J. Geng, X. J. Loh, D. Das, T.-C. Lee and O. A. Scherman, *Angew. Chem., Int. Ed*., 2012, **51**, 9633–9637.

7 (a) C. Tan, M. R. Pinto and K. S. Schanze, *Chem. Commun*., 2002, 446–447; (b) V. Stepanenko, M. Stocker, P. Müller, M. Büchner and F. Würthner, *J. Mater. Chem*., 2009, **19**, 6816–6826; (c) G. R. Whittell, M. D. Hager, U. S. Schubert and I. Manners, *Nat. Mater.*, 2011, **10**, 176–188.

8 (a) Y.-b. Lim, K.-S. Moon and M. Lee, *Chem. Soc. Rev*., 2009, **38**, 925–934; (b) C. Wang, Z. Wang and X. Zhang, *Acc. Chem. Res*., 2012, **45**, 608–618.

9 (a) J. P. Hill, W. Jin, A. Kosaka, T. Fukushima, H. Ichihara, T. Shimomura, K. Ito, T. Hashizume, N. Ishii and T. Aida, *Science*, 2004, **304**, 1481–1483; (b) J. F. Hulvat, M. Sofos, K. Tajima and S. I. Stupp, *J. Am. Chem. Soc*., 2005, **127**, 366–372; (c) B. Narayan, S. P. Senanayak, A. Jain, K. S. Narayan and S. J. George, *Adv. Funct. Mater*., 2013, **23**, 3053–3060; (d) S. Yagai, S. Okamura, Y. Nakano, M. Yamauchi, K. Kishikawa, T. Karatsu, A. Kitamura, A. Ueno, D. Kuzuhara, H. Yamada, T. Seki and H. Ito, *Nat. Commun*., 2014, **5**, 1–10; (e) C. Rest, A. Martin, V. Stepanenko, N. K. Allampally, D. Schmidt and G. Fernández, *Chem. Commun.*, 2014, **50**, 13366–13369.

10 N. C. Seeman, *J. Theor. Biol*., 1982, **99**, 237–247.

11 For reviews, see: (a) K. V. Gothelf and T. H. LaBean, *Org. Biomol. Chem*., 2005, **3**, 4023–4037; (b) N. C. Seeman, *Annu. Rev. Biochem*., 2010, **79**, 65–87; (c) F. A. Aldaye, A. L. Palmer and H. F. Sleiman, *Science*, 2008, **321**, 1795–1799; (d) A. V. Pinheiro, D. Han, W. M. Shih and H. Yan, *Nat. Nanotech*., 2011, **6**, 763–772; (e) T. Tørring, N. V. Voigt, J. Nangreave, H. Yan and K. V. Gothelf, *Chem. Soc. Rev*., 2011, **40**, 5636–5646.

12 (a) J. Gao, C. Strässler, D. Tahmassebi and E. T. Kool, *J. Am. Chem. Soc*., 2002, **124**, 11590–11591; (b) H. Kashida, H. Asanuma and M. Komiyama, *Angew. Chem., Int. Ed*., 2004, **43**, 6522–6525; (c) E. Mayer-Enthart and H.-A. Wagenknecht, *Angew. Chem., Int. Ed*., 2006, **45**, 3372–3375; (d) V. L. Malinovskii, F. Samain and R. Häner, *Angew. Chem., Int. Ed.*, 2007, **46**, 4464–4467; (f) R. Varghese and H.-A. Wagenknecht, *Chem. Commun.*, 2009, 2615–2624; (g) R. Varghese and H.-A. Wagenknecht, *Chem. Eur. J*., 2010, **16**, 9040–9046; (h) V. L. Malinovskii, D. Wenger and R. Häner, *Chem. Soc. Rev.*, 2010, **39**, 410–422.

13 (a) M. P. Thompson, M.-P. Chien, T.-H. Ku, A. M. Rush and N. C. Gianneschi, *Nano Lett*., 2010, **10**, 2690–2693; (b) K. M. M. Carneiro, F. A. Aldaye and H. F. Sleiman, *J. Am. Chem. Soc*., 2010, **132**, 679–685; (c) M. Kwak and A. Herrmann, *Chem. Soc. Rev*., 2011, **40**, 5745–5755; (d) Z. Zhao, L.Wang, Y. Liu, Z. Yang, Y.-M. He, Z. Li, Q.-H. Fan and D. Liu, *Chem. Commun.*, 2012, **48**, 9753–9755; (e) X. Xiong, H. Liu, Z. Zhao, M. B. Altman, D. Lopez-Colon, C. J. Yang, L.-J. Chang, C. Liu and W. Tan, *Angew. Chem., Int. Ed*., 2013, **52**, 1472–1476; (f) M. Humenik, M. Drechsler and T. Scheibel, *Nano Lett*., 2014, **14**, 3999–4004; C. Zhou, D. Wang, Y. Dong, L. Xin, Y. Sun, Z. Yang and D. Liu, *Small*, 2015, **11**, 1161–1164 (h) Y. Vyborna, M. Vybornyi, A. V. Rudnev and R. Häner, *Angew. Chem., Int. Ed.*, 2015, **54**, 7934–7938.

14 L. Wang, Y. Feng, Y. Sun, Z. Li, Z. Yang, Y.-M. He, Q.-H. Fan and D. Liu, *Soft Matter*, 2011, **7**, 7187–7190.

15 F. E. Alemdaroglu, K. Ding, R. Berger and A. Herrmann, *Angew. Chem., Int. Ed*., 2006, **45**, 4206–4210.

16 M.-P. Chien and N. C. Gianneschi, *Small*, 2011, **7**, 2041–2046.

17 M. Kwak, J. Gao, D. K. Prusty, A. J. Musser, V. A. Markov, N. Tombros, M. C. A. Stuart, W. R. Browne, E. J. Boekema, G. Brinke, H. T. Jonkman, B. J. van Wees, M. A. Loi and A. Herrmann, *Angew. Chem., Int. Ed.*, 2011, **50**, 3206– 3210.

18 M.-P. Chien, M. P. Thompson and N. C. Gianneschi, *Chem. Commun.*, 2011, **47**, 167–169.

19 T. G. W. Edwardson, K. M. M. Carneiro, C. K. McLaughlin, C. J. Serpell and H. F. Sleiman, *Nat. Chem*., 2013, **5**, 868–875.

20 F. E. Alemdaroglu, N. C. Alemdaroglu, P. Langguth and A. Herrmann, *Adv. Mater*., 2008, **20**, 899–902.

21 (a) S. E. Averick, S. K. Dey, D. Grahacharya, K. Matyjaszewski and S. R. Das, *Angew. Chem., Int. Ed.*, 2014, **53**, 2739–2744; (b) T. G. W. Edwardson, K. M. M. Carneiro, C. J. Serpell and H. F. Sleiman, *Angew. Chem., Int. Ed*., 2014, **53**, 4567–4571.

22 (a) J. Gierlich, G. A. Burley, P. M. E. Gramlich, D. M. Hammond and T. Carell, *Org. Lett*., 2006, **8**, 3639–3642; (b) G. Godeau, C. Staedel, P. Barthélémy, *J. Med. Chem*., 2008, **51**, 4374–4376; (c) A. H. El-Sagheera and T. Brown, *Chem. Soc. Rev*., 2010, **39**, 1388–1405; (d) C. Beyer and H.-A. Wagenknecht, *Chem. Commun*., 2010, **46**, 2230–2231; (e) S. Pal, R. Varghese, Z. Deng, Z. Zhao, A. Kumar, H. Yan and Y. Liu, *Angew. Chem., Int. Ed*., 2011, **50**, 4176–4179; (f) S. E. Averick, E. Paredes, S. K. Dey, K. M. Snyder, N. Tapinos, K. Matyjaszewski and S. R. Das, *J. Am. Chem. Soc*., 2013, **135**, 12508−12511; (g) A. Aimé, N. Beztsinna, A. Patwa, A. Pokolenko, I. Bestel, P. Barthélémy, *Bioconjugate Chem*., 2013, **24**, 1345–1355; (h) M. Humenik and T. Scheibel, *ACS Nano*, 2014, **8**, 1342–1349; (i) R. V. Thaner, I. Eryazici, O. K. Farha, C. A. Mirkin and S. T. Nguyen, *Chem. Sci.*, 2014, **5**, 1091–1096.

23 S. K. Albert, H. V. P. Thelu, M. Golla, N. Krishnan, S. Chaudhary and R. Varghese, *Angew. Chem., Int. Ed*., 2014, **53**, 8352–8357.

24 (a) A. C. Grimsdale and K. Müllen, *Angew. Chem., Int. Ed*., 2005, **44**, 5592–5629; (b) Z. Chen, A. Lohr, C. R. Saha-Möller and F. Würthner, *Chem. Soc. Rev*., 2009, **38**, 564–584.

25 D. Kim, J. Heo, S. Ham, H. Yoo, C.-H. Lee, H. Yoon, D. Ryu, D. Kim and W.-D. Jang, *Chem. Commun*., 2011, **47**, 2405–2407.

26 F. Würthner, S. Yao, T. Debaerdemaeker and R. Wortmann, *J. Am. Chem. Soc*., 2002, **124**, 9431–9447.

27 L.-A. Fendt, I. Bouamaied, S. Thöni, N. Amiot and E. Stulz, *J. Am. Chem. Soc*., 2007, **129**, 15319–15329.

28 U. Rösch, S. Yao, R. Wortmann and F. Würthner, *Angew. Chem., Int. Ed*., 2006, **45**, 7026–7030.

29 B.-S. Kim, D.-J. Hong, J. Bae and M. Lee, *J. Am. Chem. Soc*., 2005, **127**, 16333–16337.

Published on 23 May 2016. Downloaded by University College London on 24/05/2016 16:41:21.

Organic & Biomolecular Chemistry Accepted Manuscript


This journal is © The Royal Society of Chemistry 20xx

Please do not adjust margins

View Article Online
DOI: 10.1039/C6OB00681G



30 E. N. Savariar, S. V. Aathimanikandan, and S. Thayumanavan, *J. Am. Chem. Soc*., 2006, **128**, 16224–16230.
31 M. Yang, W. Wang, F. Yuan, X. Zhang, J. Li, F. Liang, B. He, B. Minch and G. Wegner, *J. Am. Chem. Soc*., 2005, **127**, 15107–15111.

Published on 23 May 2016. Downloaded by University College London on 24/05/2016 16:41:21.

Organic & Biomolecular Chemistry Accepted Manuscript



Please do not adjust margins